ARTICLE

50 nm DNA Nanoarrays Generated from Uniform Oligonucleotide Films

Hyunwoo Noh,[†,‡] Albert M. Hung,[†] Chulmin Choi,[‡,§] Ju Hun Lee,[†,‡] Jin-Yeol Kim,[‡,§] Sungho Jin,[†,‡,§] and Jennifer N. Cha[†,‡,*]

[†]Department of Nanoengineering, [‡]Materials Science and Engineering Program, and [§]Department of Mechanical and Aerospace Engineering, University of California, San Diego, 9500 Gilman Drive, M/C 0448, La Jolla, California 92093-0448

ABSTRACT One of the most challenging but potentially rewarding goals in nanoscience is the ability to direct the assembly of nanoscale materials into functional architectures with high yields, minimal steps, and inexpensive procedures. Despite their unique physical properties, the inherent difficulties of engineering wafer-level arrays of useful devices from nanoscale materials in a cost-effective manner have provided serious roadblocks toward technological impact. To address nanoscale features while still maintaining low fabrication costs, we demonstrate here an inexpensive printing method that enables repeated patterning of large-area arrays of nanoscale materials. DNA strands were patterned over 4 mm areas with 50 nm resolution by a soft-lithographic subtraction printing process, and DNA hybridization was used to direct the assembly of sub-20 nm materials to create highly ordered two-dimensional nanoparticle arrays. The entire printing and assembly process was accomplished in as few as three fabrication steps and required only a single lithographically templated silicon master that could be used repeatedly. The low-cost procedures developed to generate nanoscale DNA patterns can be easily extended toward roll-to-roll assembly of nanoscale materials with sub-50 nm resolution and fidelity.

KEYWORDS: DNA · nanopatterning · self-assembly

In recent years, a wealth of nanoscale materials has demonstrated unique physical characteristics with the potential to yield enormous societal benefits, particularly toward health and energy.[1−17] However, challenges in fabricating devices from these materials over large areas, reproducibly, cheaply, and with high fidelity have hindered their widespread application. This is due primarily to the difficulties in parallel manipulation of large quantities of individual components whose dimensions are well below 10 nm and organizing them into configurations that are amenable to device and circuit wiring. Conventional patterning approaches based on lithography have to date been limited to defining relatively large-area features that result in the deposition of poorly organized ensembles of these nanostructures, thus compromising their performance.

In light of some of these challenges, self-assembling biological systems such as DNA and protein arrays have been investigated to address sub-20 nm scale materials.[18−31] The beauty of biological templates is that these systems provide immediate access to the sub-10 nm regime, and biomolecular recognition can be used to accurately position particular sets of nanoscale objects at will. For example, DNA- and protein-based self-assembled arrays have been used to build discrete assemblies of gold and semiconductor nanocrystals into two-dimensional patterns.[21−24,27−29] Despite these single demonstrations, however, production of highly parallel arrays of nanoscale materials over very large areas has not yet been shown. In fact, methods to generate large-area assemblies of nanoparticles have only recently been demonstrated with the discovery and implementation of finite 100 nm DNA structures, known as DNA origami.[32] However, in all of these studies, the DNA scaffolds had to be assembled on substrates patterned by electron-beam lithography, which is highly time-consuming and expensive (unpublished data).

In the aforementioned studies, the initial primary challenge was to accurately place and direct the assembly of the DNA strands and structures themselves on surfaces. One of the best known and least expensive methods to fabricate patterned DNA arrays is microcontact printing (μCP), but the inherent difficulties of generating poly(dimethylsiloxane) (PDMS) stamps with submicrometer dimensions have hindered attempts to pattern DNA below 500 nm. More recently, Wang and co-workers used poly(methylmethacrylate) (PMMA) stamps that were prepared first by nanoimprint lithography (NIL) to generate 250 nm lines of covalently attached single-stranded DNA (ssDNA) on silicon.[33] Stellacci and Crooks also independently developed a replica-based stamping approach starting from patterned ssDNA covalently attached on

*Address correspondence to jencha@ucsd.edu.

Received for review May 28, 2009 and accepted July 08, 2009.

Published online July 14, 2009.
10.1021/nn900559m CCC: $40.75

surfaces to generate daughter patterns of ssDNA on other substrates.[34,35] Obtaining DNA patterns with submicrometer dimensions has yet to be achieved using a simple stamping approach that obviates repeated use of lithography tooling such as NIL or photolithography or the need for chemical attachment of DNA to surfaces.

Recently, Delamarche and co-workers developed a facile "subtraction printing" method to fabricate large-area antibody arrays with 100 nm resolution.[36] While proteins have directed the assembly of nanocrystals, issues of protein stamping and stability make them difficult and expensive to use for nanoscale assembly. Since DNA can be further used to direct the assembly of nanoscale materials, we investigated this technique to create arrays of linear ssDNA of varying dimensions.

The general scheme of using the subtraction printing method for obtaining clean patterns of ssDNA on silicon and native oxide is shown in Figure 1. In subtraction printing, material is transferred from flat PDMS to a patterned silicon master only where there is conformal contact between the DNA film and the silicon surface, but not where there are etched holes or trenches in the silicon substrate. This leaves behind patterned DNA arrays on the flat PDMS that are subsequently transferred ("printed") by contact with a planar silicon or oxide surface. While this had been clearly demonstrated with antibodies in the earlier work, the basic chemical and physical differences between that of DNA and proteins required significant optimization for successful inking of DNA on PDMS and transfer to silicon.

One of the predominant criteria to obtain well-defined patterns of DNA or proteins through subtraction-based PDMS stamping is the optimization of adhesion between the biomolecules and the PDMS surface relative to the receiving surface.[37,38] Because the PDMS surface is much more hydrophobic than cleaned oxide or glass substrates, it can sometimes be difficult to obtain conformal wetting and adhesion of charged, hydrophilic species, like DNA, to the PDMS substrate. For both μCP and subtraction printing, a certain amount of adherence between DNA and PDMS is needed to avoid dewetting or delamination. For subtraction printing, sufficient adhesion between the DNA and the silicon surface is absolutely necessary because the process requires complete transfer of DNA from the PDMS upon contact, whereas partial transfer can sometimes be sufficient for μCP. Another major challenge with printing hydrophilic species is controlling the amount of water in the system in order to prevent excess flow of the biomolecules while still allowing for material transfer.

Due to the highly charged nature of both single- and double-stranded DNA and high levels of hydration, the issue of flow proved to be a significant challenge toward obtaining proper subtraction and printing of DNA films on PDMS even after removal of excess solvent by spin-coating or nitrogen drying. In initial studies, a standard published procedure for biomolecule inking on PDMS

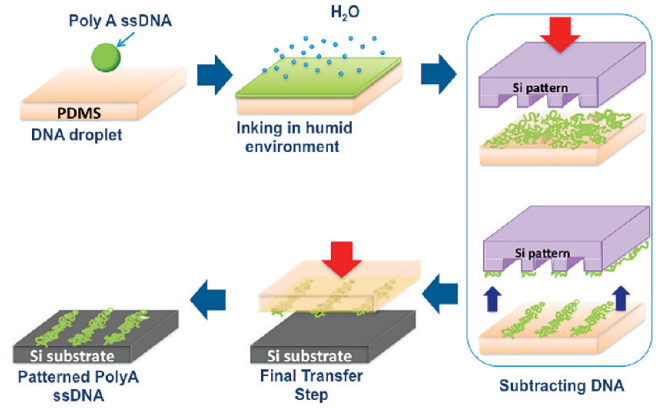

Figure 1. Schematic depicting method of DNA adsorption to planar PDMS and subtraction printing to generate patterns of ssDNA on silicon. Solutions of ssDNA were first adsorbed and slowly evaporated on UV/ozone-treated planar PDMS substrates. After drying in a humidified environment for ~45 min, the DNA films were brought into conformal contact with UV/ozone-treated lithographically patterned silicon masters. After subtraction printing, patterned ssDNA domains remained behind on the planar PDMS, which were then transferred to flat silicon substrates.

was used where DNA solutions were first incubated on the PDMS substrates for varied amounts of time followed by nitrogen blow-drying for a few seconds. The DNA solutions used in these experiments varied in magnesium concentrations ranging from 0 to 125 mM $MgCl_2$, and both untreated and UV/ozone-treated PDMS substrates were tested. However, in all cases, DNA solution inking on PDMS followed by nitrogen drying or spin-coating yielded both poor pattern fidelity (Figure 2) as well as the negative tone of the expected patterns. This was the case regardless of DNA concentration, magnesium concentration, inking time, pretreatment of the silicon substrates with magnesium solutions, surface oxidation of PDMS by UV/ozone, or spin-coating speeds. We hypothesize that the large hydration sphere around the DNA strands increases DNA mobility, causing the adsorbed DNA strands to act as a fluid and essentially flow into the etched domains of the silicon substrate, leaving behind any excess DNA on PDMS as a DNA film with micrometer-sized holes. In contrast, when DNA solutions were completely dried on the PDMS stamps, no DNA was observed to transfer from the PDMS surface to either the patterned or planar silicon substrates. In light of both of these results, it became clear that, although excess solvent must be removed from the adsorbed DNA film, the DNA strands also needed to remain partially hydrated in order for effective transfer from PDMS to silicon to occur.

As a means to both address issues of DNA flow as well as effective transfer from PDMS to silicon, DNA solutions of varying concentrations were left to slowly evaporate on the flat PDMS surfaces in a humidified environment. The reason for this setup was to reproducibly control the evaporation speed of the DNA solutions on PDMS. A critical component of the subtraction printing process required DNA films that contained no visible excess water but were hydrated enough to allow

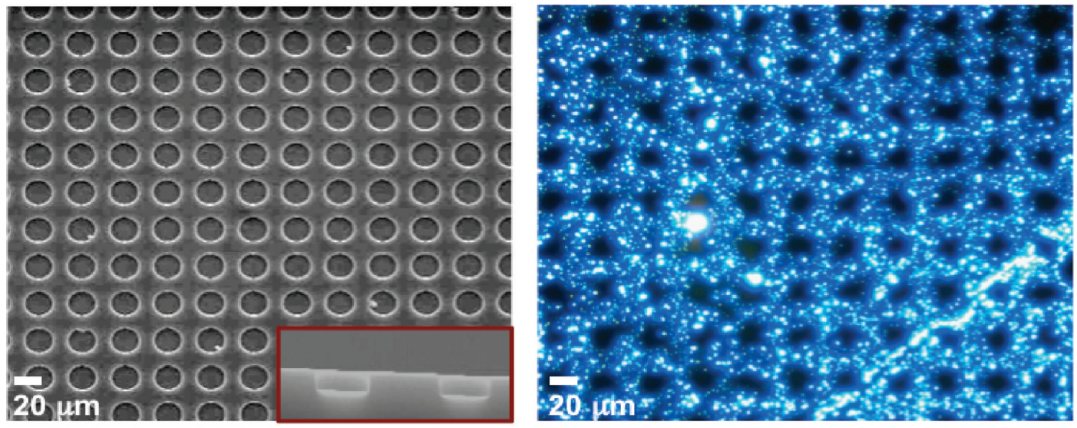

Figure 2. (A) SEM image of 20 μm holes etched into silicon. (B) Fluorescence image of DNA patterns generated using 20 μm silicon master when DNA was inked onto the PDMS by nitrogen blow-drying DNA solutions preadsorbed onto the PDMS substrates.

for effective transfer, and these were most reproducibly obtained by slow evaporation of the DNA solutions on PDMS in Petri dishes lined with Kimwipes. A sample procedure is as follows: 20 pmol (1 μL) of ssDNA was spread onto 3 mm × 4 mm PDMS substrates and left for 45 min in a humidified chamber built from Petri dishes lined with wet Kimwipes (Figure 1). Immediately after solvent evaporation (45 min), all of the samples were treated briefly with a nitrogen flow for 5−10 s and brought into conformal contact with UV/ozone-treated lithographically patterned and etched silicon substrates. Any DNA patterns generated by subtraction printing and left on the flat PDMS substrates were next brought into a second conformal contact with planar, UV/ozone-treated silicon substrates (Figure 1). As shown in Figure 3, silicon masters with 5 and 1 μm holes could be used to generate 5 and 1 μm dot patterns of single-stranded DNA (ssDNA), polyadenine, A_{15}, on flat silicon.

Next, sub-1 μm silicon masters generated by deep UV lithography (DUV) were used to measure the scalability of the patterns that could be generated. By using the exact same patterning steps as for the larger micrometer-size patterns, ssDNA domains as small as 100 nm were repeatedly patterned on silicon with excellent fidelity. Both ssDNA dots and lines as small as 95 nm were also generated (Figure 4), illustrating effective pattern transfer regardless of shape. Even smaller features were obtained by placing silicon line patterns made by DUV lithography in a conventional resistive heating furnace to oxidize in O_2 (99%) for 3 h at 1000 °C, then etched to form sub-50 nm lines. These were then replicated by NIL into PMMA resists, which were used as an etching mask to faithfully transfer the patterns into Si wafer by a SF_6/C_4F_8 mixture RIE, achieving 40 nm wide trenches in silicon. As shown in Figure 5a, these silicon masters could be used to obtain 40−50 nm lines of ssDNA with ease. Finally, the ease and mildness of the subtraction printing process prevents the removal or degradation of the previously deposited ssDNA, allowing for multiple patterning of different ssDNA sequences into complex patterns. Specifically, grid-like, 100 nm line patterns of ssDNA were produced by performing two sequential printing steps at right angles to one another (Figure 5b).

While there was some variability of DNA film thickness across the PDMS substrate, this did not appear to cause visible differences in the overall fidelity of the DNA patterns obtained on the receiving silicon surface. As determined by AFM height measurements, each domain was approximately 5 nm in height, correlating to an approximate film thickness of 1−2 strands of A_{15} DNA oligonucleotides. If it is assumed that a 15mer ssDNA is ~5 nm when fully extended, then one can assume that at least a single monolayer of ssDNA is patterned. However, since ssDNA is known to often coil and form condensed and globular structures,[39] it is more likely that multiple layers of ssDNA are patterned on the silicon surface after printing. Regardless, any ssDNA not directly adsorbed to the silicon surface would be washed away in either water or buffer, leaving behind only a monolayer of ssDNA on the substrate. Indeed, since no covalent chemistry was employed in these studies to directly conjugate the DNA to the silicon surface, much of the adsorbed and patterned ssDNA domains were observed to completely wash away with repeated water rinses. However, high magnesium buffer (125 mM $MgCl_2$) was found to prevent the complete disassociation of the ssDNA from the silicon surface.[40] This use of magnesium became a critical aspect when using the patterned DNA for directing nanoparticle assembly. In order to generalize this process for nanomaterials sensitive to excess magnesium, methods to covalently conjugate the ssDNA to silicon after transfer from PDMS are currently being investigated.

The ability to generate 50 nm features of ssDNA over macroscopic areas repeatedly and with minimal lithogra-

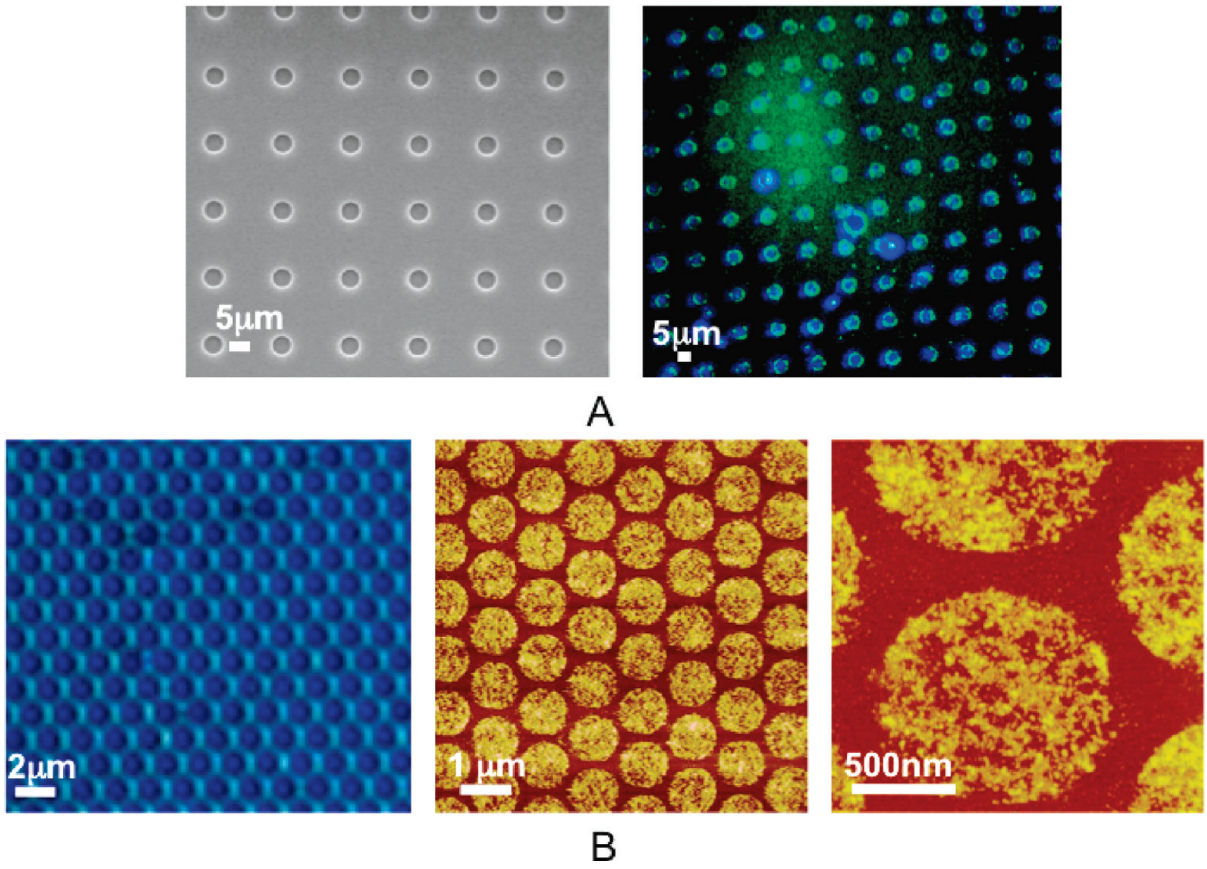

Figure 3. (A) Etched holes (5 μm) in silicon and dot patterns (5 μm) of fluorescently tagged polyadenine (A_{15}). (B) Optical micrograph of 1 μm holes etched in silicon and AFM height images of 1 μm dot patterns of polyadenine obtained after subtraction printing from the silicon master.

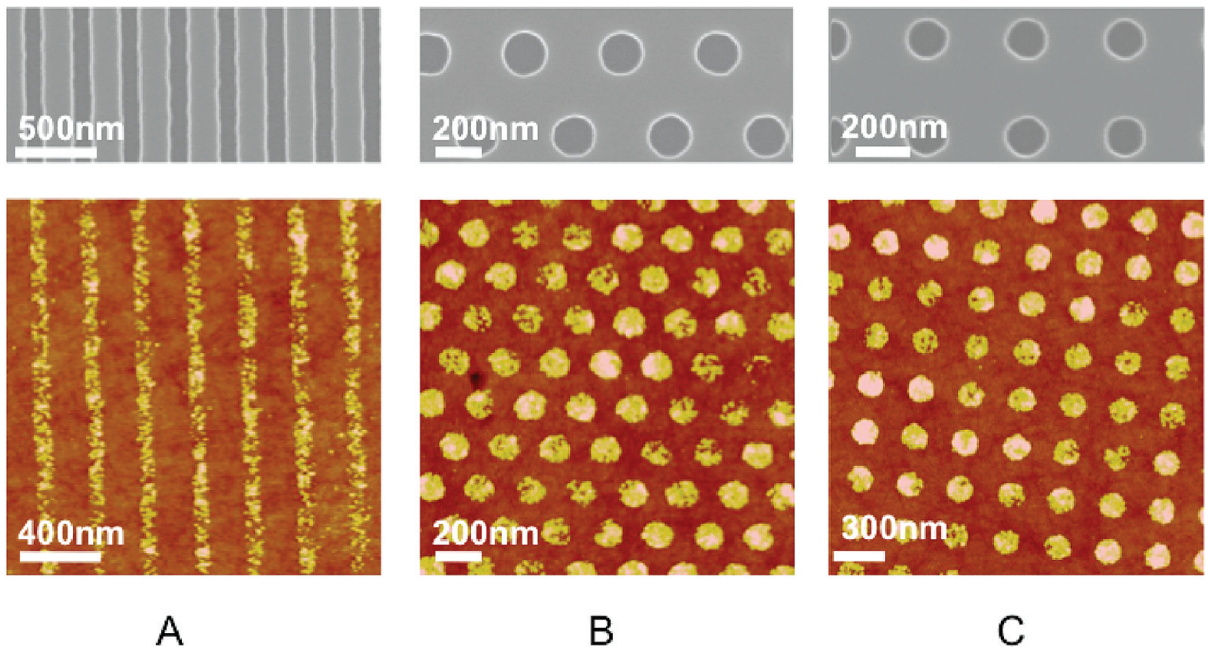

Figure 4. (A) Etched lines (~100 nm) in silicon and lines of ssDNA (95 nm) generated after subtraction printing of DNA films with the 100 nm silicon patterns. (B) Etched holes (180 nm) in silicon and dot patterns (180 nm) of ssDNA. (C) Etched holes (160 nm, square array) in silicon and dot patterns (160−170 nm, square array) of ssDNA generated.

phy or complex chemistry provides a means to direct the assembly of nanoscale materials at low cost and with a limited number of fabrication steps. The assembly of gold nanocrystals onto lines of printed ssDNA through DNA hybridization is demonstrated here. Specifically, 10 nm gold nanocrystals modified with polythymine (T_{15})

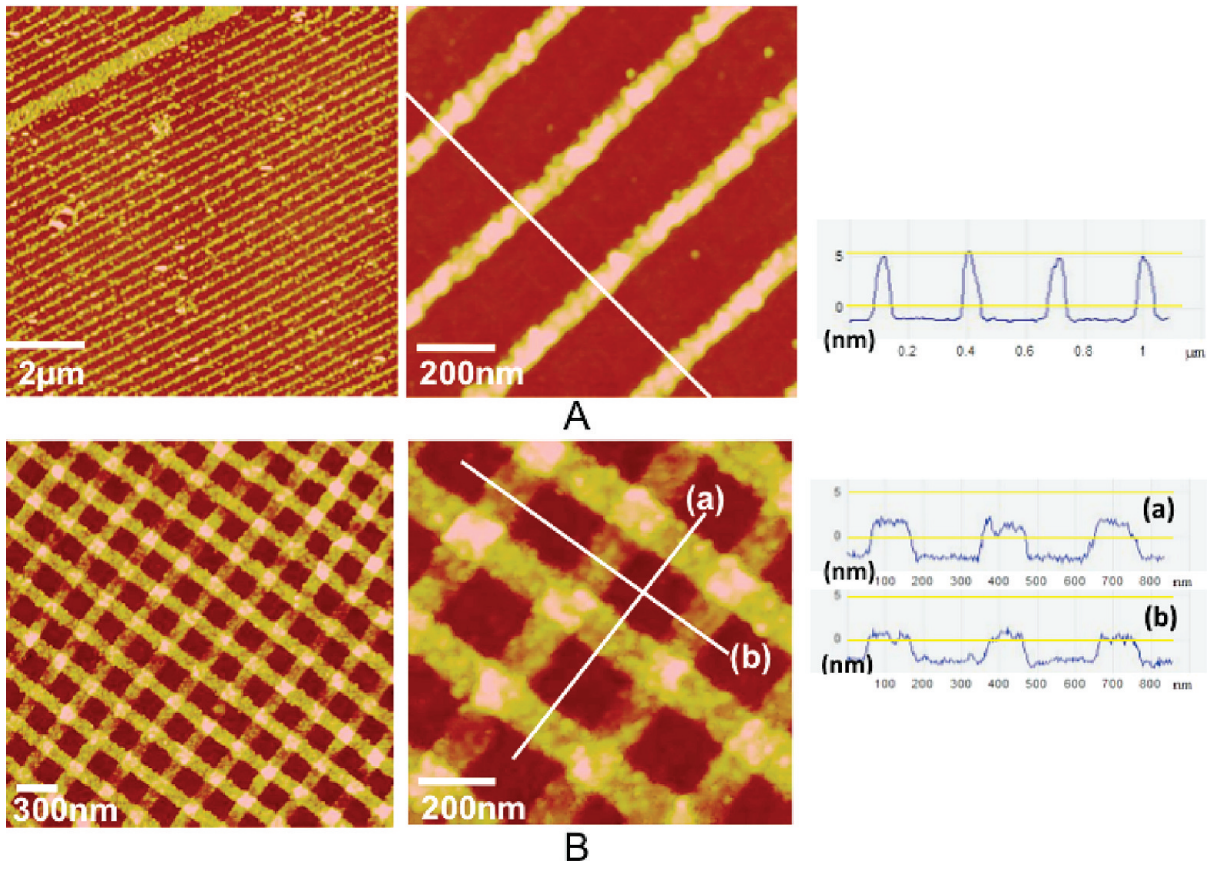

Figure 5. (A, Left) Large-area AFM image of 50 nm DNA lines obtained after subtraction printing. (Right) AFM images of 50 nm DNA lines obtained after subtraction printing and height profile analysis. (B, Left) AFM images of 100 nm crossed lines of ssDNA. (Right) Higher magnification AFM image of 100 nm crossed lines of ssDNA and height profile analysis.

were reacted at room temperature in magnesium buffer for 5 min with 50 nm patterned lines of A_{15}. After adsorption of the gold nanocrystal solutions, the substrate was quickly immersed in a fresh bath of Tris-acetate-EDTA (TAE) buffer with 125 mM $MgCl_2$ to wash away excess, unbound gold nanocrystals. Next, the samples were introduced to solutions of 50% ethanol (v/v) and 50% water to wash away excess magnesium and finally immersed in 90% ethanol for 20 min to remove excess water and effectively dry the nanocrystals to the patterned DNA lines. As shown in Figure 6, the patterned ssDNA remained on the surface after introduction of new solutions of T_{15} conjugated 10 nm gold nanoparticles. All of the gold nanocrystals appeared to hybridize to the A_{15} sites in a matter of minutes, and extended incubation did not appear to cause a substantial difference in the number of nanoparticles bound. Furthermore, when ssDNA lines were annealed at room temperature with solutions of DNA-conjugated gold nanocrystals, two-dimensional, close-packed arrays of gold nanoparticles were obtained with observed hierarchical ordering of the gold colloids themselves (Figure 6b,c). Although the printed ssDNA lines were measured to be between 50 and 60 nm in width, the assembled gold nanocrystal lines varied in widths from 60 to ~100 nm. The differences in the widths of the printed ssDNA lines from the nanocrystal line patterns are presumed to occur due to nanocrystal hybridization that can occur at the edges of the ssDNA domains. When 100 nm crossed line patterns of A_{15} were exposed to the T_{15}-conjugated 10 nm gold nanocrystals, continuous arrays of nanoparticles were obtained that clearly followed the DNA crossed line patterns (Figure 6d). The ability to obtain long-range order of nanocolloids by confining the particles to sub-100 nm domains can clearly be applied toward fabrication of useful photonic, electronic, and magnetic devices and will be of future study.

We have demonstrated here a facile method to produce submicrometer features of ssDNA that allow the arrangement of a wide variety of nanoscopic components over macroscopic areas. The strengths of this approach are its versatility, ease of fabrication, and minimization of lithographic tooling and processes. Furthermore, the resulting nanometer scale chemical patterns allow not only the directed placement of nanoscale materials but also the investigation of the role of chemical confinement in creating complex assembled arrays. Finally, mild conditions used in the stamping process will facilitate the fabrication of three-dimensional nanoscale assemblies routinely and predictably over large areas, a feat that has been difficult to achieve with current technologies.

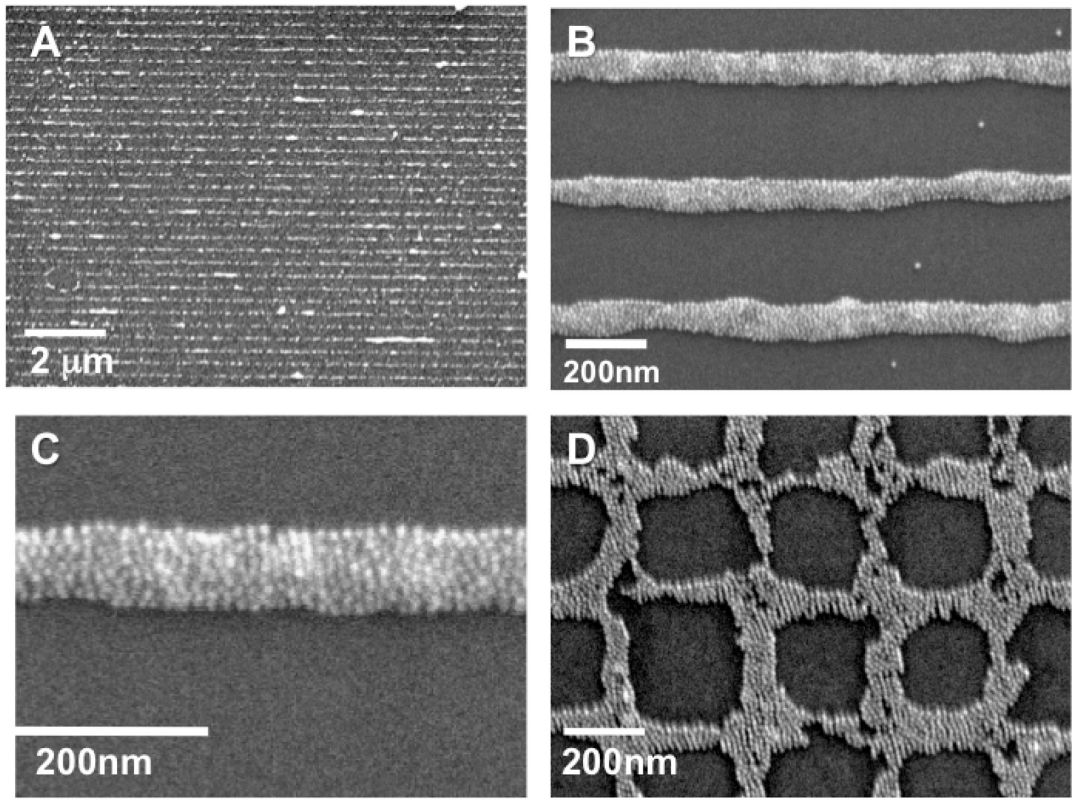

Figure 6. (A) Thymine (T_{15})-conjugated 10 nm gold nanocrystals annealed to ~50−60 nm polyadenine (A_{15}) patterned lines on silicon. (B,C) Higher magnification image of gold nanocrystal assemblies showing two-dimensional nanoparticle packing within the 60−100 nm nanocrystal line patterns. (D) Gold nanocrystal assemblies on 100 nm crossed lines of polyadenine (A_{15}).

MATERIALS AND METHODS

PDMS Preparation. PDMS substrates (Sylgard 184, Dow Corning) were prepared by mixing and degassing a mixture of base and curing agent (ratio 10:1). PDMS liquid was poured into a Petri dish and then thermally cured at 80 °C in an oven for 1 h.

Silicon Masters. The silicon masters were fabricated on (100) silicon wafers patterned with 193 nm deep ultraviolet (DUV) lithography and a reactive-ion-etch (RIE) process with an oxide hardmask. Approximately 100 nm thick SiO_2 was deposited on 300 mm diameter silicon wafers in an Applied Materials 5000 plasma enhanced chemical vapor deposition (PE-CVD) system using tetraethoxysilane (TEOS) chemistry. A UV-sensitive high-resolution photoresist was then spin-coated on the silicon wafers. An antireflective (AR) coating was applied on top of the resist to eliminate standing waves in the photoresist. The DUV lithography was performed on an ASML/SVGL Micrascan 193 nm step-and-scan lithography system. The resist was developed, and the fine lithographic features were transferred with high fidelity by RIE etching first into the oxide layer to create the hard-mask and then into the silicon substrate. The SiO_2 was etched with fluorine-based chemistry in an Applied Materials Centura 5200 etcher, and the silicon was etched with chlorine-based chemistry in a LAM Rainbow 9400PTX etcher.

Silicon Masters with Sub-50 nm Dimensions. Original line patterns (120 nm) generated by DUV lithography were placed in a conventional resistive heating furnace and oxidized in pure O_2 (99%) for 3 h at 1000 °C, with optional chemical etching of the oxide layer to form the pillar pattern with sub-50 nm width for nanoimprint. The Si template was then replicated by imprinting onto a poly(methylmethacrylate) (PMMA)-coated silicon wafer using an ANT-2 nanoimprinter. After transferring the pattern into the substrate, PMMA was used as an etching mask to faithfully transfer the patterns into Si wafer by a SF_6/C_4F_8 mixture RIE, achieving a sub-50 nm wide line hole.

DNA Patterning. Si master and planar Si substrates were cleaned with acetone, ethanol, and DI water successively using a sonication bath. PDMS substrates were treated with ethanol and DI water successively using a sonication bath. After cleaning, both the silicon and PDMS substrates were treated with a UVO cleaner (Jelight, model 42) for 1 h under 3 scfh oxygen gas.

UVO-cleaned PDMS substrates were inked with 1 μL of 20 μM amine-modified polyadenine and incubated in a Petri dish lined with wet Kimwipes for 45 min. The DNA-inked PDMS was then briefly treated with nitrogen gas for 5−10 s. Both the subtraction and printing steps were done using 50 g weights and using 30 s transfer times.

Gold Nanoparticle Conjugation. Phosphine-stabilized 10 nm gold nanocrystals (Ted Pella) were reacted with 5′-thiolated polythymine (T_{15}) using ratios of 200:1 DNA to gold. After a minimum of 1 h, excess DNA was removed by microcentrifuge filtration and gel electrophoresis was run to confirm DNA to gold conjugation. T_{15}-modified gold nanocrystal solutions were reacted at room temperature for 5 min with the patterned A_{15}. After adsorption of the gold nanocrystal solutions, all of the substrates were quickly immersed in a bath (1× TAE buffer) of 125 mM $MgCl_2$ for 2 s to wash away excess gold nanocrystals. Next, the samples were introduced to a solution of 50% ethanol in water (v/v) for ~2 s and then immersed in 90% ethanol to wash away excess salts and dehydrate the DNA.

Characterization. SEM images were obtained with Phillips XL30 ESEM. All images in this paper were taken with a secondary electron mode. The accelerating voltage was 20 kV. Tapping mode AFM images were obtained using Digital Instrument MultiMode Nanoscope IV with an "E" scanner and using Ultrasharp AFM tips.

Acknowledgment. The authors thank Dr. Andrew Goodwin for manuscript editing, and Ryan Anderson and Dr. Maribel Montero for their training and assistance with the microscopy and cleanroom instrumentation. This work is financially sup-

ported by the Office of Naval Research (Award Number N00014-09-01-0250) and UCSD startup funds.

REFERENCES AND NOTES

1. Lu, W.; Lieber, C. M. Nanoelectronics from the Bottom up. *Nat. Mater.* **2007**, *6*, 841–850.
2. Huang, Y.; Duan, X.; Wei, Q.; Lieber, C. M. Directed Assembly of One-Dimensional Nanostructures into Functional Networks. *Science* **2001**, *291*, 630–633.
3. Rueckes, T.; Kim, K.; Joselevich, E.; Tseng, G. Y.; Cheung, C.-L.; Lieber, C. M. Carbon Nanotube-Based Nonvolatile Random Access Memory for Molecular Computing. *Science* **2000**, *289*, 94–97.
4. McEuen, P. L.; Fuhrer, M. S.; Park, H. Single-Walled Carbon Nanotube Electronics. *IEEE Trans. Nanotechnol.* **2002**, *2*, 78–85.
5. Lieber, C. M. Nanoscale Science and Technology: Building a Big Future from Small Things. *Mater. Res. Soc. Bull.* **2003**, *28*, 486–491.
6. Cheng, M. M.-C.; Cuda, G.; Bunimovich, Y. L.; Gaspari, M.; Heath, J. R.; Hill, H. D.; Mirkin, C. A.; Nijdam, A. J.; Terracchiano, R.; Thundat, T.; Ferrari, M. Nanotechnologies for Biomolecular Detection and Medical Diagnostics. *Curr. Opin. Chem. Biol.* **2006**, *10*, 11–19.
7. Taton, T. A.; Mirkin, C. A.; Letsinger, R. L. Scanometric DNA Array Detection with Nanoparticle Probes. *Science* **2000**, *289*, 1757–1760.
8. Cui, Y.; Wei, Q.; Park, H.; Lieber, C. M. Nanowire Nanosensors for Highly Sensitive and Selective Detection of Biological and Chemical Species. *Science* **2001**, *293*, 1289–1292.
9. McAlpine, M. C.; Ahmad, H.; Wang, D.; Heath, J. R. Highly Ordered Nanowire Arrays on Plastic Substrates for Ultrasensitive Flexible Chemical Sensors. *Nat. Mater.* **2007**, *6*, 379–384.
10. Xu, J. M. Plastic Electronics and Future Trends in Microelectronics. *Synth. Met.* **2000**, *115*, 1–3.
11. Ferrari, M. Cancer Nanotechnology: Opportunities and Challenges. *Nat. Rev. Cancer* **2005**, *5*, 161–171.
12. Thundat, T.; Majumdar, A. Microcantilevers for Physical, Chemical, and Biological Sensing. *Sensors Sensing Biol. Eng.* **2003**, 338–355.
13. Chaudhary, S.; Lu, H.; Müller, A. M.; Bardeen, C. J.; Ozkan, M. Hierarchical Placement and Associated Optoelectronic Impact of Carbon Nanotubes in Polymer-Fullerene Solar Cells. *Nano Lett.* **2007**, *7*, 1973–1979.
14. Beek, W. J. E.; Wienk, M. M.; Janssen, R. A. J. Efficient Hybrid Solar Cells from Zinc Oxide Nanoparticles and a Conjugated Polymer. *Adv. Mater.* **2004**, *16*, 1009–1013.
15. Huynh, W. U.; Dittmer, J. J.; Alivisatos, A. P. Hybrid Nanorod-Polymer Solar Cells. *Science* **2002**, *295*, 2425–2427.
16. Gur, I.; Fromer, N. A.; Geier, M. L.; Alivisatos, A. P. Air-Stable All-Inorganic Nanocrystal Solar Cells Processed from Solution. *Science* **2005**, *310*, 462–465.
17. Law, M.; Greene, L. E.; Johnson, J. C.; Saykally, R. J.; Yang, P. Nanowire Dye-Sensitized Solar Cells. *Nat. Mater.* **2005**, *4*, 455–459.
18. Seeman, N. C.; Belcher, A. M. Emulating Biology: Building Nanostructures from the Bottom up. *Proc. Natl. Acad. Sci. U.S.A.* **2002**, *99*, 6451–6455.
19. Claridge, S. A.; Liang, H. W.; Basu, S. R.; Fréchet, J. M. J.; Alivisatos, A. P. Isolation of Discrete Nanoparticle−DNA Conjugates for Plasmonic Applications. *Nano Lett.* **2008**, *8*, 1202–1206.
20. Fu, A. H.; Micheel, C. M.; Cha, J.; Chang, H.; Yang, H.; Alivisatos, A. P. Discrete Nanostructures of Quantum Dots/Au with DNA. *J. Am. Chem. Soc.* **2004**, *126*, 10832–10833.
21. Le, J. D.; Pinto, Y.; Seeman, N. C.; Musier-Forsyth, K.; Taton, T. A.; Kiehl, R. A. DNA-Templated Self-Assembly of Metallic Nanocomponent Arrays on a Surface. *Nano Lett.* **2004**, *4*, 2343–2347.
22. Deng, Z.; Tian, Y.; Lee, S.-H.; Ribbe, A. E.; Mao, C. DNA-Encoded Self-Assembly of Gold Nanoparticles into One-Dimensional Arrays. *Angew. Chem., Int. Ed.* **2005**, *44*, 3582–3585.
23. Zhang, J.; Liu, Y.; Ke, Y.; Yan, H. Periodic Square-like Gold Nanoparticle Arrays Templated by Self-Assembled 2D DNA Nanogrids on a Surface. *Nano Lett.* **2006**, *6*, 248–251.
24. Alivisatos, A. P.; Johnsson, K. P.; Peng, X.; Wilson, T. E.; Loweth, C. J.; Bruchez, M. P.; Schultz, P. G. Organization of 'Nanocrystal Molecules' Using DNA. *Nature* **1996**, *382*, 609–611.
25. Aldaye, F. A.; Palmer, A. L.; Sleiman, H. F. Assembling Materials with DNA as the Guide. *Science* **2008**, *321*, 1795–1799.
26. Seeman, N. C. DNA in a Material World. *Nature* **2003**, *421*, 427–431.
27. Yan, H.; Park, S. H.; Finkelstein, G.; Reif, J. H.; LaBean, T. H. DNA-Templated Self-Assembly of Protein Arrays and Highly Conductive Nanowires. *Science* **2003**, *301*, 1882–1884.
28. McMillan, R. A.; Paavola, C. D.; Howard, J.; Chan, S. L.; Zaluzec, N. J.; Trent, J. D. Ordered Nanoparticle Arrays Formed on Engineered Chaperonin Protein Templates. *Nat. Mater.* **2002**, *1*, 247–252.
29. Dieluweit, S.; Pum, D.; Sleytr, U. B.; Kautek, W. Monodisperse Gold Nanoparticles Formed on Bacterial Crystalline Surface Layers (S-Layers) by Electroless Deposition. *Mater. Sci. Eng., C* **2005**, *25*, 727–732.
30. Mao, C.; Solis, D. J.; Reiss, B. D.; Kottman, S. T.; Sweeney, R. Y.; Hayhurst, A.; Georgiou, G.; Iverson, B.; Belcher, A. M. Virus-Based Toolkit for the Directed Synthesis of Magnetic and Semiconducting Nanowires. *Science* **2004**, *303*, 213–217.
31. Lee, S.-W.; Mao, C.; Flynn, C. E.; Belcher, A. M. Ordering of Quantum Dots Using Genetically Engineered Viruses. *Science* **2002**, *296*, 892–895.
32. Rothemund, P. W. K. Folding DNA to Create Nanoscale Shapes and Patterns. *Nature* **2006**, *440*, 297–302.
33. Wang, Y.; Goh, S. H.; Bi, X.; Yang, K.-L. Replication of DNA Submicron Patterns by combining Nanoimprint Lithography and Contact Printing. *J. Colloid Interface Sci.* **2009**, *333*, 188–194.
34. Yu, A. A.; Savas, T. A.; Taylor, G. S.; Guiseppe-Elie, A.; Smith, H. I.; Stellacci, F. Supramolecular Nanostamping: Using DNA as Movable Type. *Nano Lett.* **2005**, *5*, 1061–1064.
35. Lin, H.; Kim, J.; Sun, L.; Crooks, R. M. Replication of DNA Microarrays from Zip Code Masters. *J. Am. Chem. Soc.* **2006**, *128*, 3268–3272.
36. Coyer, S. R.; García, A. J.; Delamarche, E. Facile Preparation of Complex Protein Architectures with Sub-100-nm Resolution on Surfaces. *Angew. Chem., Int. Ed.* **2007**, *46*, 6837–6840.
37. Lange, S. A.; Benes, V.; Kern, D. P.; Hörber, J. K. H.; Bernard, A. Microcontact Printing of DNA Molecules. *Anal. Chem.* **2004**, *76*, 1641–1647.
38. Guan, J.; Lee, L. J. Generating Highly Ordered DNA Nanostrand Arrays. *Proc. Natl. Acad. Sci. U.S.A.* **2005**, *102*, 18321–18325.
39. Washizu, M.; Kimura, Y.; Kobayashi, T.; Kurosawa, O.; Matsumoto, S.; Mamine, T. Stretching DNA as a Template for Molecular Construction. *AIP Conf. Proc.* **2004**, *725*, 67–76.
40. Pastre, D.; Hamon, L.; Landousy, F.; Sorel, I.; David, M. O.; Zozime, A.; Le Cam, E.; Pietrement, O. Anionic Polyelectrolyte Adsorption on Mica Mediated by Multivalent Cations: A Solution to DNA Imaging by Atomic Force Microscopy under High Ionic Strengths. *Langmuir* **2006**, *22*, 6651–6660.